Available online at www.sciencedirect.com

ScienceDirect

Ceramics International 40 (2014) 4827–4831

CERAMICS INTERNATIONAL

www.elsevier.com/locate/ceramint

Green chemistry approach for the synthesis of ZnO nanopowders and their cytotoxic effects

Majid Darroudi[a,b,*], Zahra Sabouri[c], Reza Kazemi Oskuee[b,d], Ali Khorsand Zak[e], Hadi Kargar[c], Mohamad Hasnul Naim Abd Hamid[f]

[a]*Nuclear Medicine Research Center, School of Medicine, Mashhad University of Medical Sciences, Mashhad, Iran*
[b]*Department of Modern Sciences and Technologies, School of Medicine, Mashhad University of Medical Sciences, Mashhad, Iran*
[c]*Chemistry Department, Payame Noor University, 19395-4697 Tehran, Iran*
[d]*Targeted Drug Delivery Research Center, School of Pharmacy, Mashhad University of Medical Sciences, Mashhad, Iran*
[e]*Nanotechnology Laboratory, Esfarayen University, North Khorasan, Iran*
[f]*Center for Research & Instrumentation Management, Universiti Kebangsaan Malaysia, 43600 UKM Bangi, Selangor D.E., Malaysia*

Received 21 August 2013; received in revised form 9 September 2013; accepted 9 September 2013
Available online 16 September 2013

Abstract

The use of natural polymers in the synthesis of nanomaterials can have a low cost and eco-friendly approach. In this work we would like to report the "***green chemistry***" synthesis of ZnO nanopowders (ZnO-NPs) using gelatin. Spherical ZnO-NPs were synthesized at different calcination temperatures and field emission scanning electron microscopy (FESEM) imaging showed the formation of most of nanopowders in nanoscale. The powder X-ray diffraction (PXRD) analysis revealed wurtzite hexagonal ZnO with preferential orientation at (101) reflection plane. *In vitro* cytotoxicity studies on neuro2A cells, a dose dependent toxicity with non-toxic effect of concentration below $\sim 2\ \mu g/mL$ was shown. The synthesis of ZnO-NPs in gelatinous media were found to be comparable to those obtained from the conventional reduction methods using hazardous polymers or surfactants which can be an excellent alternative for the synthesis of ZnO-NPs using biomaterials.

Keywords: A. Sol–gel processes; B. Electron microscopy; D: ZnO

1. Introduction

Zinc oxide nanopowders (ZnO-NPs) are an important metal oxide due to its interesting properties and wide applications in various fields. Nanosized ZnO particles are an important inorganic semiconductor material with a hexagonal wurtzite crystal structure which has a wide and direct band gap (nearly 3.37 eV) and large excitonic binding energy (60 meV) at ambient temperature [1,2]. The ZnO-NPs has numerous applications such as catalysis [3], piezoelectric devices [4], pigment [5], chemical sensors [6], and cosmetic materials especially for transparent UV protection [7]. There are wide reports available on the preparation of ZnO-NPs using different methodological approaches like solvothermal and hydrothermal synthesis [8–10], precipitation [11,12], polymerization method [13], laser ablation [14], sonochemical [15,16], and sol–gel [17–19] methods. However, utility of such methods suffers several drawbacks like use of high temperature and pressure, toxic reagents, long reaction time, requirement of external additives as a specific stabilizer, base and promoter during the reaction which limits purity of the final product. It is important to prepare ZnO-NPs by a simple, low cost, and eco-friendly process that has potential to yield nanoparticles of uniform particles in size. The sol–gel method has gained lots of interest among researchers since it offers controlled consolidation, shape modulation, patterning of the nanostructures and low processing temperature [20,21].

Recently, biomaterials have been used in synthesis of ZnO-NPs such as plant extracts and derivatives [22–26]. Natural polymers such as gelatin, starch, and different proteins are all

*Corresponding author at: Nuclear Medicine Research Center, School of Medicine, Mashhad University of Medical Sciences, Mashhad, Iran.
Tel.: +98 5118002286; fax: +98 511 8002287.
E-mail addresses: majiddarroudi@gmail.com, darroudim@mums.ac.ir (M. Darroudi).

0272-8842/$ - see front matter
http://dx.doi.org/10.1016/j.ceramint.2013.09.032

interesting materials in synthesis of nanomaterials because they are biodegradable and bioabsorbable with degradation products that are non-toxic [27–29]. Gelatin (GL) is a natural biopolymer extracted from the partial hydrolysis of collagen which has good biocompatibility and biodegradability, as it has been widely used in wound dressings, drug carriers, and tissue scaffolds in recent years [30]. In this study, we demonstrate a sol–gel method using GL to synthesize ZnO-NPs. Zinc nitrate was used as the zinc source at different calcination temperatures. The synthesized samples were then characterized using FESEM, XRD, TGA/DTA, FT-IR, and UV–vis spectroscopy. The majority of this research has investigated synthesis of nanoparticles in natural protein media, proving that this method is eco-friendly, low cost, and can consequently be used as an economic and valuable alternative for the large-scale production of metal and metal oxide nanoparticles.

2. Materials and methods

2.1. Materials and reagents

All the materials used were of analytical grade and were used without any purification. Zinc nitrate was purchased from Merck (Germany). Gelatin (GL, type B) was purchased from Sigma-Aldrich (USA). All glassware used in the laboratory experiments were cleaned with a fresh solution of HNO_3/HCl (3:1, v/v), washed thoroughly with doubly distilled water, and dried before use. Double distilled water was used in all experiments.

2.2. Synthesis of ZnO-NPs

To prepare 1.5 g of ZnO-NPs, 4.5 g of $Zn(NO_3)_2 \bullet 6H_2O$ was dissolved in 10 mL of distilled water and then stirred for 30 min. Meanwhile, 0.2 g of GL was dissolved in 40 mL of distilled water and stirred for 10 min at 40 °C to achieve a clear GL solution. After that, the zinc nitrate solution was added to the GL solution, and the container was moved to an oil bath. The temperature of the oil bath was fixed at 60 °C. Stirring was continued for 12 h to obtain a light brown color resin. The final product was then divided to four parts and calcined at different temperatures (400, 500, 600 and 700 °C) in air for 1 h to obtain ZnO-NPs.

2.3. Characterization of ZnO-NPs

The prepared ZnO-NPs were characterized by PXRD (Philips, X'pert, Cu Kα), FTIR (ST-IR\ST-SIR spectrometer), TGA (Q600), UV–vis (Evolution 300® Thermo Fisher Scientific), and FESEM (Carl Zeiss Supra 55VP).

2.4. Evaluation of neurotoxicity effect

The cytotoxicity of nanoparticles was evaluated by the method using 3-(4,5-dimethylthiazol-2-yl)-2,5-diphenylte-trazolium bromide (MTT) assay [31]. Briefly, neuro2A cells were seeded at a density of 1×10^4 cells per well in 96-well plates and incubated for 24 h. Thereafter, the cells were treated with various concentrations of nanoparticles in the presence of 10% FBS. The calcined ZnO-NPs at 600 °C was suspended in a stock solution at 5 μg/mL in a solution of dimethyl sulfoxide (DMSO)/double distilled water. After 24 h of incubation, 20 μl of 5 mg/mL MTT in the PBS buffer was added to each well, and the cells were further incubated for 4 h at 37 °C. The medium containing unreacted dye was discarded, and 100 μl of DMSO was added to dissolve the formazan crystal formed by live cells. Optical absorbance was measured at 590 nm (reference wavelength 630 nm) using a microplate reader (Statfax-2100, Awareness Technology, USA), and cell viability was expressed as a percent relative to untreated control cells. Values of metabolic activity are presented as mean $\pm$ SD of triplicates.

3. Results and discussion

This section reports the results of synthesized ZnO-NPs in gelatinous media. In this study, we attempted the fabrication of ZnO-NPs using the sol–gel method and GL as a green stabilizer. The extensive number of hydroxyl and amine groups present in GL molecular structure can facilitate the complexation of zinc cations (Zn^{2+}) to an initial molecular matrix. This structure enables GL to coat and stabilize zinc species and finally ZnO-NPs while inhibiting their excessive aggregation or crystal growth. As shown in Fig. 1, the color of sol–gel derived ZnO-NPs due to the increased calcination temperature changed from black to white.

The thermogravimetric and derivative analysis (TGA/DTA) curves of the as-prepared gel by the sol–gel method in a GL environment are presented in Fig. 2. The heating process was started at 20 °C, and then increased up to 490 °C with a temperature rate change of 10 °C/min. The TGA curve descends until it becomes horizontal around 490 °C, and about 77% weight loss was observed during the heating process. The TGA/DTA traces show three main regions. The first weight loss between 20 and 175 °C (17%) is an initial loss of water, bend Ed1. The second weight loss from 175 °C to 185 °C (45%) is attributed to the decomposition of chemically bound groups, which corresponds to bend Ed2. The third step from 185 to 490 °C (15%) is related to the formation of the pyrochlore phases and decomposition of the pyrochlore phases and the formation of ZnO pure phases indicated by bend Ed3.

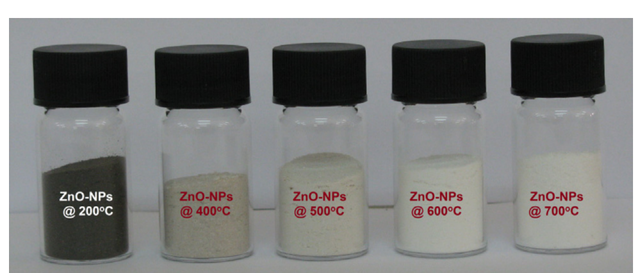

Fig. 1. Photograph of synthesized ZnO-NPs at different calcination temperatures.

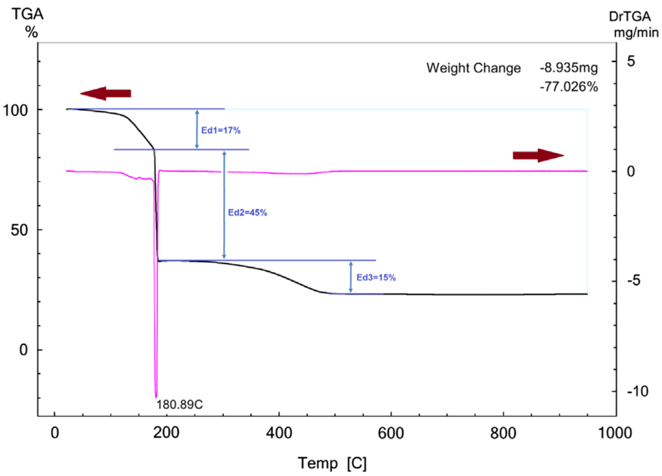

Fig. 2. The TGA/DTA curves of initial gel from 20 °C to 950 °C. It shows about 77% loss weight in three steps to achieve ZnO-NPs.

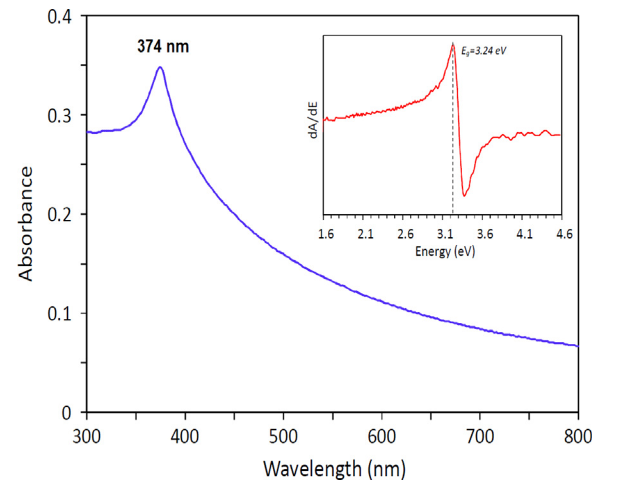

Fig. 4. UV–vis spectrum and band gap estimation (inset) of prepared ZnO-NPs at 600 °C.

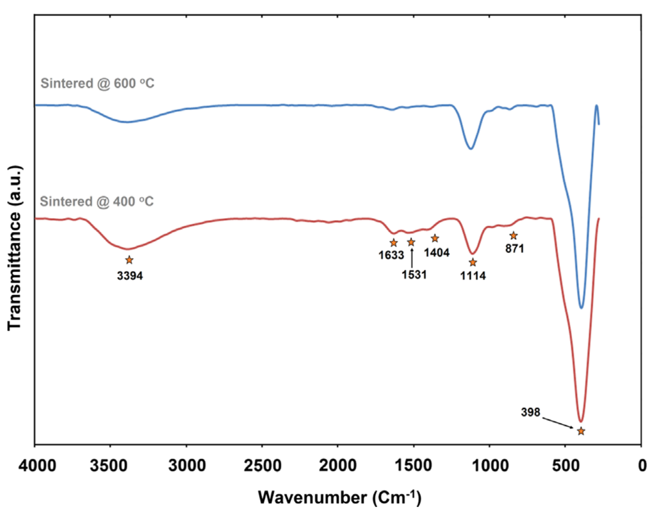

Fig. 3. FTIR spectra of the ZnO-NPs prepared at different calcination temperatures. The absorption band related to Zn–O vibration mode was clearly observed at about 400 cm^{-1}.

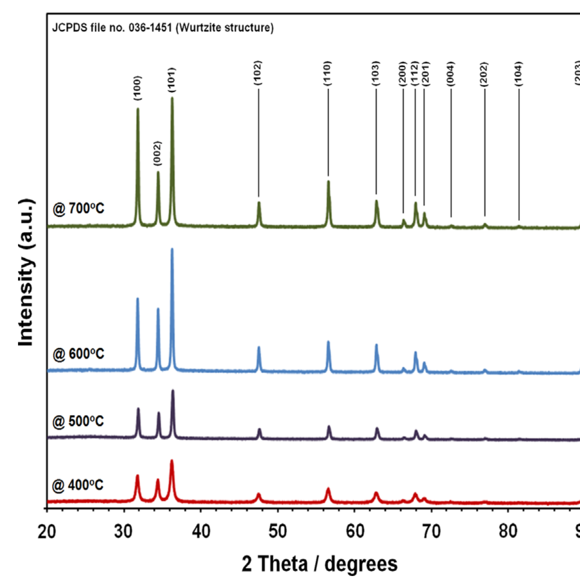

Fig. 5. The PXRD patterns of synthesized ZnO-NPs in air at different temperatures.

No weight loss between 490 and 950 °C was detected on the TGA curve, which indicates the formation of nanocrystalline ZnO as the decomposition product. Compare to our previous works, the pure phase is obtained at lower temperature [17,19].

Fig. 3 shows the FTIR spectra of the ZnO-NPs calcined at 400 and 600 °C. For the FTIR spectra of the calcined samples a series of absorption peaks from 1000 to 4000 cm^{-1} can be found, which correspond to the carboxylate and hydroxyl impurities in the sample. More specifically, the broad band at 3394 cm^{-1} was assigned to the O–H stretching mode of the hydroxyl group. The peaks observed at 1633, 1531, 1404, and 871 cm^{-1} are due to the asymmetrical and symmetrical stretching of the zinc carboxylate [32]. As shown in the FTIR traces, the spectral signatures of carboxylate impurities disappear as the calcination temperature increases (600 °C). This indicates the possibility of zinc carboxylate dissociation and conversion to ZnO during the calcination process. For both of the samples in this study, a broad absorption band was observed at around 398 cm^{-1}. The band at 398 cm^{-1} corresponds to the E_2 mode of hexagonal ZnO (Raman active) [33]. There was also an absorption band at around 1114 cm^{-1} is related to C–O and therefore can be neglected.

The room temperature UV–vis absorption spectrum of the ZnO-NPs is shown in Fig. 4. The ZnO-NPs were dispersed in water with concentration of 0.1 wt% and then the solution was used to perform the UV–vis measurement. The spectrum reveals a characteristic absorption peak of ZnO at wavelength of 374 nm which can be assigned to the intrinsic band-gap absorption of ZnO due to the electron transitions from the valence band to the conduction band ($O_{2p} \rightarrow Zn_{3d}$) [19,34]. In addition, this sharp peak shows that the particles are in nano-size, and the particle size distribution is narrow. It is clearly shown that the maximum peak in the absorbance spectrum does not correspond to the true optical band gap of the ZnO-NPs. A common way to obtain the band gap from absorbance spectra is to get the first derivative of the absorbance with respect to photon energy and find the maximum in the derivative spectrum at the lower energy sides [35,36]. The derivative of the absorbance of the ZnO-NPs is shown in the inset of Fig. 4, and it indicates a band gap of 3.24 eV for the ZnO-NPs. The good absorption of the ZnO-NPs in the UV region proves the applicability of this product in such medical application such as sun-screen protectors or as antiseptic in ointments [37].

The PXRD patterns of the ZnO-NPs calcined at different temperatures of 400, 500, and 600, 700 °C are shown in Fig. 5. All of the detectable peaks with Miller indices (100), (002), (101), (102), (110), (103), (200), (112), (201), (004), (202), (104), and (203) can be indexed to the ZnO wurtzite structure (JCPDS #036-1451). The broadening of the peaks indicates that the crystalline size are in nanoscale [38] and this result indicates that the size of the obtained samples is fine and small which confirmed by the FEEM images at different magnifications of prepared ZnO-NPs at 600 °C (Fig. 6). High homogeneity of prepared ZnO-NPs in GL media was confirmed as well as by FESEM images (Fig. 6). The as-prepared ZnO-NPs were calcined at different temperatures for 1 h, PXRD peaks become sharper with increasing calcination temperatures and FWHM decreased, indicating that the crystallinity of ZnO-NPs is accelerated by the calcination process. Moreover, no other peaks related to an impurity for prepared ZnO-NPs at different calcination temperatures, indicating that the final nanopowders were relatively pure.

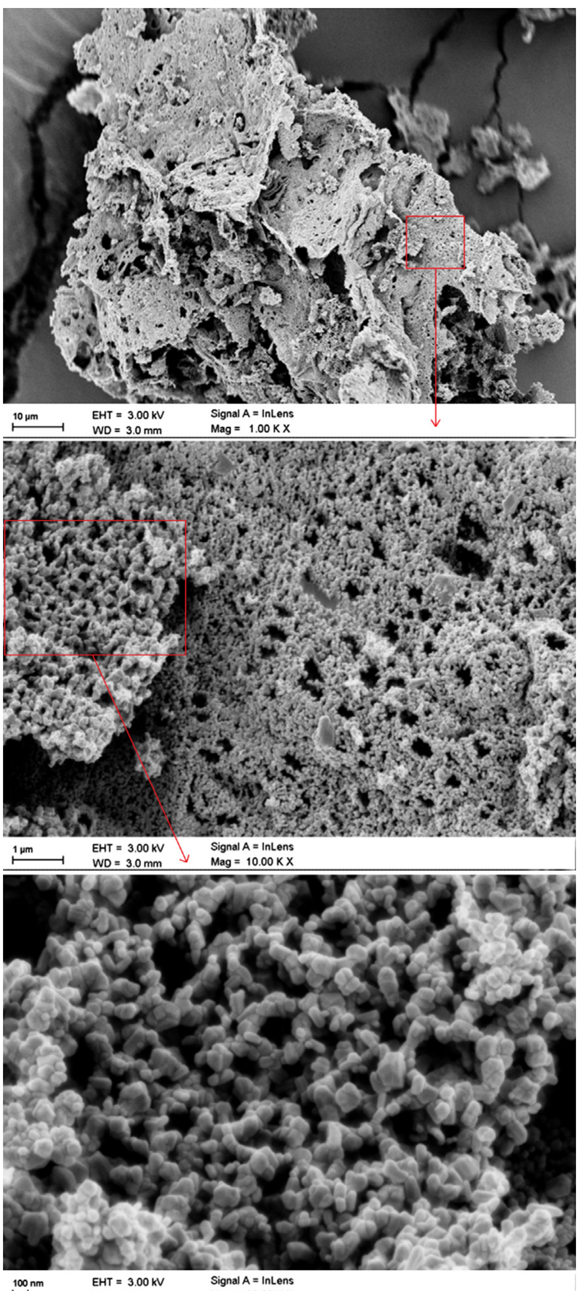

Fig. 6. FESEM images at different magnifications of prepared ZnO-NPs at 600 °C.

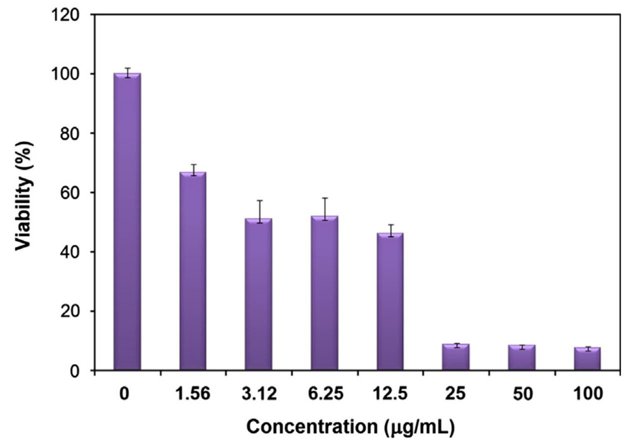

Fig. 7. Cell viability of neuro2A cells measured by the MTT assay. Cells were incubated for 24 h with the indicated concentrations of the nanoparticles.

The results of *in vitro* cytotoxicity studies after 24 h of incubation with different concentrations of nanoparticles, ranging from 0 to 100 μg/mL, are shown in Fig. 7. As the results showed, for concentration above 2 μg/mL the metabolic activity was decreased in a concentration dependent manner meaning that metabolic activity started to decrease from 2 μg/mL and at 100 μg/mL maximal decrease was observed.

4. Conclusion

ZnO-NPs were synthesized by the sol–gel method in GL as a bio-polymeric template. From XRD results, it was observed that all of the ZnO-NPs calcined at different temperatures exhibited the high purity with the hexagonal (wurtzite) structure. The typical band gap was estimated from UV–vis spectrum and was obtained to be about 3.24 eV. This method is interesting for applying and extending the green chemistry rules in preparation of nanoparticles such as simple and low cost synthesis in a normal atmosphere without any special physical conditions. It is expected that these nanoparticles can find potential applications in different fields such as cosmetics and optical/electrical devices as well as medicinal applications.

References

[1] Z. Deng, M. Chen, G. Gu, L. Wu, A facile method to fabricate ZnO hollow spheres and their photocatalytic property, Journal of Physical Chemistry B 112 (2008) 16–22.

[2] Z.L. Wang, ZnO nanowire and nanobelt platform for nanotechnology, Materials Science & Engineering R: Reports 64 (2009) 33–71.

[3] W.F. Elseviers, H. Verelst, Transition metal oxides for hot gas desulphurization, Fuel 78 (1999) 601–612.

[4] S. Fujihara, H. Naito, T. Kimura, Visible photoluminescence of ZnO nanoparticles dispersed in highly transparent MgF_2 thin-films via sol–gel process, Thin Solid Films 389 (2001) 227–232.

[5] F.A. Sigoli, M.R. Davolos, M. Jafelicci, Morphological evolution of zinc oxide originating from zinc hydroxide carbonate, Journal of Alloys and Compounds 262 (1997) 292–295.

[6] R. Mochinaga, T. Yamasaki, T. Arakawa, The gas sensing of $SmCoO_x$/MO_x (M=Fe, Zn, In, and Sn) having a heterojunction, Sensors and Actuators B: Chemical 52 (1998) 96–99.

[7] H. Akiyama, O. Yamasaki, H. Kanzaki, J. Tadaa, J. Arata, Effects of zinc oxide on the attachment of *Staphylococcus aureus* strains, Journal of Dermatological Science 17 (1998) 67–74.

[8] R. Razali, A.K. Zak, W.H.A. Majid, M. Darroudi, Solvothermal synthesis of microsphere ZnO nanostructures in DEA media, Ceramics International 37 (8) (2011) 3657–3663.

[9] Q. Li, Z. Kang, B. Mao, E. Wang, C. Wang, C. Tian, S. Li, One-step polyoxometalate-assisted solvothermal synthesis of ZnO microspheres and their photoluminescence properties, Materials Letters 62 (2008) 2531–2534.

[10] H.Y. Xu, H. Wang, Y.C. Zhang, W.L. He, M.K. Zhu, B. Wang, H. Yan, Hydrothermal synthesis of zinc oxide powders with controllable morphology, Ceramics International 30 (2004) 93–97.

[11] C.L. Kuo, C.L. Wang, H.H. Ko, W.S. Hwang, K.M. Chang, W.L. Li, H.H. Huang, Y.H. Chang, M.C. Wang, Synthesis of zinc oxide nanocrystalline powders for cosmetic applications, Ceramics International 36 (2010) 693–698.

[12] R. Song, Y. Liu, L. He, Synthesis and characterization of mercaptoacetic acid modified ZnO nanoparticles, Solid State Science 10 (2008) 1563–1567.

[13] P. Jajarmi, Fabrication of pure ZnO nanoparticles by polymerization method, Materials Letters 63 (2009) 2646–2648.

[14] R. Zamiri, A. Zakaria, H.A. Ahangar, M. Darroudi, A.K. Zak, G.P.C. Drummen, Aqueous starch as a stabilizer in zinc oxide nanoparticle synthesis via laser ablation, Journal of Alloys and Compounds 516 (2012) 41–48.

[15] C. Deng, H. Hu, G. Shao, C. Han, Facile template-free sonochemical fabrication of hollow ZnO spherical structures, Materials Letters 64 (2010) 852–855.

[16] A. Khorsand Zak, W.H.A. Majid, H.Z. Wang, Ramin Yousefi, A. Moradi Golsheikh, Z.F. Ren, Sonochemical synthesis of hierarchical ZnO nanostructures, Ultrasonics Sonochemistry 20 (2013) 395–400.

[17] A.K. Zak, W.H.A. Majid, M. Darroudi, R. Yousefi, Synthesis and characterization of ZnO nanoparticles prepared in gelatin media, Materials Letters 65 (2011) 70–73.

[18] F. Bigdeli, A. Morsali, Synthesis ZnO nanoparticles from a new zinc (II) coordination polymer precursor, Materials Letters 64 (2010) 4–5.

[19] A. Khorsand Zak, W.H. Abd. Majid, M.R. Mahmoudian, Majid Darroudi, Ramin Yousefi, Starch-stabilized synthesis of ZnO nanopowders at low temperature and optical properties study, Advanced Powder Technology 24 (2013) 618–624.

[20] B. Sunandan, D. Joydeep, Hydrothermal growth of ZnO nanostructures, Science and Technology of Advanced Materials 10 (2009) 013001.

[21] E.G. Lori, D.Y. Benjamin, L. Matt, Z. David, Y. Peidong, Solution grown zinc oxide nanowires, Inorganic Chemistry 45 (2006) 7535–7543.

[22] N.A. Samat, R.M. Nor, Sol–gel synthesis of zinc oxide nanoparticles using *Citrus aurantifolia* extracts, Ceramics International 39 (2013) S545–S548.

[23] G. Sangeetha, S. Rajeshwari, R. Venckatesh, Green synthesis of zinc oxide nanoparticles by *Aloe barbadensis* miller leaf extract: structure and optical properties, Materials Research Bulletin 46 (2011) 2560–2566.

[24] R.P. Singh, V.K. Shukla, R.S. Yadav, P.K. Sharma, P.K. Singh, A.C. Pandey, Biological approach of zinc oxide nanoparticles formation and its characterization, Advanced Materials Letters 2 (2011) 313–317.

[25] V. Rana, P. Rai, A.K. Tiwary, R.S. Singh, J.F. Kennedy, C.J. Knill, Modified gums: approaches and applications in drug delivery, Carbohydrate Polymers 83 (2011) 1031–1047.

[26] M. Darroudi, Z. Sabouri, R. Kazemi Oskuee, A. Khorsand Zak, H. Kargar, M.H.N.Abd Hamid, Sol–gel synthesis, characterization, and neurotoxicity effect of zinc oxide nanoparticles using gum tragacanth, Ceramics International 39 (2013) 9195–9199.

[27] M. Darroudi, M.B. Ahmad, R. Zamiri, A.K. Zak, A.H. Abdullah, N.A. Ibrahim, Time-dependent effect in green synthesis of silver nanoparticles, International Journal of Nanomedicine 6 (2011) 677–681.

[28] M. Darroudi, M. Sarani, R. Kazemi Oskuee, A. Khorsand Zak, H.A. Hosseini, L. Gholami, Green synthesis and evaluation of metabolic activity of starch mediated nanoceria, Ceramics International (2013) (in press).

[29] M.R. Mozafari, Nanomaterials and Nanosystems for Bi Applications, Springer, Dordrecth, 2007.

[30] X. Xu, M. Zhou, Antimicrobial gelatin nanofibers containing silver nanoparticles, Fibers and Polymers 9 (2008) 685–690.

[31] T. Mosmann, Rapid colorimetric assay for cellular growth and survival: application to proliferation and cytotoxicity assays, Journal of Immunological Methods 65 (1983) 55–63.

[32] G. Xiong, U. Pal, J.G. Serrano, K.B. Ucer, R.T. Williams, Photoluminesence and FTIR study of ZnO nanoparticles: the impurity and defect perspective, Physica Status Solidi C 3 (2006) 3577–3581.

[33] A. Kaschner, U. Haboeck, M. Strassburg, M. Strassburg, G. Kaczmarczyk, A. Hoffmann, C. Thomsen, A. Zeuner, H.R. Alves, D.M. Hofmann, B. K. Meyer, Nitrogen-related local vibrational modes in ZnO:N, Applied Physics Letters 80 (2002) 1909–1911.

[34] A. Khorsand Zak, R. Yousefi, W.H.A. Majid, M.R. Muhamad, Facile synthesis and X-ray peak broadening studies of $Zn_{1-x}Mg_xO$ nanoparticles, Ceramics International 38 (2012) 2059–2064.

[35] A. Khorsand Zak, R. Razali, W.H.A. Majid, M. Darroudi, Synthesis and characterization of a narrow size distribution of zinc oxide nanoparticles, International Journal of Nanomedicine 6 (2011) 1399–1403.

[36] M. Darroudi, M. Hakimi, M. Sarani, R. Kazemi Oskuee, A. Khorsand Zak, L. Gholami, Facile synthesis, characterization, and evaluation of neurotoxicity effect of cerium oxide nanoparticles, Ceramics International 39 (2013) 6917–6921.

[37] F. Harding, Breast Cancer: Cause–Prevention–Cure, Tekline Publishing, Aylesbury, 2006.

[38] B. Djuricic, S. Pickering, Nanostructured cerium oxide: preparation and properties of weakly-agglomerated powders, Journal of the European Ceramic Society 19 (1999) 1925–1934.